

Stabilization by a Divalent Transition Metal in Lead Indium Quaternary Selenide, $\text{Fe}_{0.47}\text{Pb}_{8.04}\text{In}_{17.37}\text{Se}_{34}$, and Specific Indium Coordination

Yoshitaka Matsushita,^{*,†,‡} Kazumasa Sugiyama,[‡] and Yutaka Ueda[†]

Institute for Solid State Physics (ISSP), The University of Tokyo, 5-1-5 Kashiwanoha, Kashiwa, Chiba 277-8581, Japan, Department of Earth & Planetary Science, The University of Tokyo, 7-3-1 Hongo, Bunkyo-ku, Tokyo 113-0033, Japan, and Neutron Scattering Team, Quantum Beam Center, National Institute for Material Science (NIMS), 1-1 Namiki, Tsukuba, Ibaraki, 305-0044 Japan

Received June 26, 2006

Single crystals of the first M–Pb–In–Se quaternary selenide, $\text{Fe}_{0.47}\text{Pb}_{8.04}\text{In}_{17.37}\text{Se}_{34}$, with the structure stabilized by a divalent transition metal ($M = \text{Fe}$), have been grown by a solid-state reaction. The Fe^{II} ions partially occupy at the In sites with various Fe/In ratios. Thus, a new crystal structure is evolved by partially occupied minor Fe atoms at In sites. A part of the In atoms shows remarkably distorted octahedral coordination. This compound shows relatively high conductivity (~ 40 S/m at 300 K) with a narrow-band-gap-type semiconducting property ($E_a = 0.078$ eV).

Recently, the research of transition-metal chalcogenides has been revived in solid-state chemistry because the chalcogenides have various kinds of specific physical properties and are in a wide variety for applied materials in the next generation, such as thermoelectric materials,¹ nonlinear optical materials,² photoelectric materials,³ phosphors,⁴ and solid-state electrolytes for Li secondary batteries.⁵ In addition to applications, chalcogenides are also important in fields of basic sciences such as magnetochemistry and magneto-physics. We have studied a multinary chalcogenide system containing transition metals in anticipation of an exciting new magnetophenomena. Many of chalcogenides have local dimensionalities caused by environments of the elements, because the dimensionality of the framework structures or doping level can control the ratio of the cation to chalcogen atom in chalcogenides, as has been achieved in oxides.⁶ Especially, we had focused on chalcogenides having a one-

dimensional Heisenberg antiferromagnetic (1D-HAF) chain structure because most of them are considered as a prototype in static physics.⁷ Recently, we reported the crystal structure and physical properties of a rare $S = 2$ 1D-HAF compound, $\text{FePb}_4\text{Sb}_6\text{S}_{14}$. The magnetic susceptibility of this compound shows a broad maximum, indicating short magnetic ordering around 33.5 K, and a spin-glass behavior at the lower temperature range.⁸

Moreover, in very recent years, Lee and our group independently found out that a small amount of the transition metals (M) partially is substituted in the In sites in the “Pb–In–S” system. This substitution effect evolves the new crystal structure types.^{9,10} In other words, M acts as a stabilizer element for those new structures. In this paper, we describe the crystal structure and physical properties of the new compound, $\text{Fe}_{0.47}\text{Pb}_{8.04}\text{In}_{17.37}\text{Se}_{34}$ (hereafter, **1**). This is the first selenide example that is structurally stabilized by a divalent transition metal.

1 crystals were grown by a solid-state reaction in an evacuated silica tube.¹¹ Needle-shaped black crystals with shiny metallic luster were obtained with a small amount of byproducts such as orthorhombic $\text{Pb}_{7.12}\text{In}_{18.88}\text{Se}_{34}$,¹² PbIn_2Se_4 ,¹³ and PbSe . The chemical composition of the selected crystal was estimated by the results of energy-dispersive

- (6) Eichhorn, B. W. *Prog. Inorg. Chem.* **1994**, *42*, 139.
 (7) Katsumata, K. *Curr. Opin. Solid State Mater. Sci.* **1997**, *2*, 226.
 (8) (a) Matsushita, Y.; Ueda, Y. *Inorg. Chem.* **2003**, *42*, 7830. (b) Matsushita, Y.; Ueda, Y. *Prog. Theor. Phys. Suppl.* **2005**, *159*, 179.
 (9) Matsushita, Y.; Ueda, Y. *Inorg. Chem.* **2006**, *45*, 2022.
 (10) Wang, K.-C.; Lee, C.-S. *Inorg. Chem.* **2006**, *45*, 1415.

(11) All manipulations were performed in air. **1** crystals have been obtained by a solid-state reaction using Fe (3N, Power), PbSe , In_2Se_3 (3N, Lump), and Se (4N, Shot). PbSe was synthesized for 36 h under evacuated conditions from Pb (4N, Shot) and Se, and these raw materials were heated at 773 K for 36 h under evacuated conditions. Fe was reduced by pure H_2 gas at 1073 K for 5 h before use. These starting materials were expeditiously mixed in the molar ratio of Fe: $\text{PbSe}:\text{In}_2\text{Se}_3:\text{Se} = 1.5:5.5:5:1.5$ in air. The mixture sealed into an evacuated silica tube (10^{-5} Torr), was slowly heated to 1173 K over 12 h, isothermed at this temperature for 72 h, cooled to 673 K over 100 h, and then cooled to room temperature within 10 h. The homogeneity of prepared samples was checked by powder XRD using a MacScience M21X (Cu $K\alpha$ radiation, 45 kV, 350 mA).

* To whom correspondence should be addressed. E-mail: chaos_ym@yahoo.co.jp.

[†] Institute for Solid State Physics (ISSP), The University of Tokyo.

[‡] Quantum Beam Center, National Institute for Material Science (NIMS).

- (1) Kanatzidis, M. G. *Semicond. Semimet.* **2001**, *69*, 51.
 (2) Liao, J.-H.; Marking, G. M.; Hsu, K.-F.; Matsushita, Y.; Ewbank, M. D.; Borwick, R.; Cunningham, P.; Rosker, M. J.; Kanatzidis, M. G. *J. Am. Chem. Soc.* **2003**, *125*, 9484.
 (3) Ibuki, S.; Yoshimatsu, S. *J. Phys. Soc. Jpn.* **1955**, *10*, 549.
 (4) Shionoya, S.; Yen, W. M., Eds. *Phosphor Handbook*; CRC Press: Boca Raton, FL, 1999.
 (5) (a) Matsushita, Y.; Kanatzidis, M. G. *Z. Naturforsch.* **1998**, *53b*, 23. (b) Kanno, R.; Hata, T.; Kawamoto, Y.; Irie, M. *Solid State Ionics* **2000**, *130*, 97.

spectrometry (EDS) at $\text{Fe}_{0.49}\text{Pb}_{8.05}\text{In}_{17.51}\text{Se}_{34}$ from an average value of 20 different positions on a crystal.¹⁴ From the results of differential thermal analysis (DTA) measurements, the melting and recrystallizing points of this compound were determined at 987 and 951 K, respectively.¹⁵ X-ray diffraction (XRD) results of the final product show the same pattern as the starting material. This suggests that this compound exhibits a congruent melt. This compound does not appear in the reported pseudobinary $\text{PbSe}-\text{In}_2\text{Se}_3$ phase diagram.¹³ To identify the effect of the introduction of Fe, we also tried to synthesize the pseudobinary region ($0.375 > \text{PbSe}/\text{In}_2\text{Se}_3 > 0.5625$) without Fe atoms, but we could not observe any isostructural phase as **1**. Therefore, Fe is an essential element to form the crystal structure of **1**.

A single crystal of compound **1** having approximate dimensions $0.1 \times 0.1 \times 0.2$ mm for the crystal structure determination was selected under a microscope.¹⁶ This crystal is as the same as the sample using EDS analyses. The basic structure is an isostructure with $\text{M}^+\text{Pb}_8\text{In}_{17}\text{S}_{34}$ ($\text{M}^+ = \text{Cu}, \text{Ag}, \text{Au}$; hereafter **2**),¹⁰ and all of the atoms locate at the 2e Wyckoff position in $P2_1/m$. The refined structural composition is $\text{Fe}_{0.47(9)}\text{Pb}_{8.02(6)}\text{In}_{17.37(9)}\text{Se}_{34}$.¹⁷ This composition is exactly consistent with the results of EDS measurement. The structure is formed by three $\text{PbSe} (= \text{NaCl})$ -related slabs (A–C) elongated to the a direction (Figure S1). A similar building mode between these slabs is also observed in the $\text{In}_2\text{Sn}_3\text{S}_7$ structure.¹⁸ The slabs A and C formed by In and Se atoms are an isostructure, which is based on the ribbon structure having the PbSe^{111} unit. One In tetrahedron (In2 in slab A and In8 in slab C) connects the unit of three In polyhedrons arranged with different directions. The coordination type of In atoms in these slabs (In1–2 and In8–9) is nearly regular octahedral coordination with the range of average In–Se distance 2.744–2.767 Å (Figure 1a). On the other hand, the slab B formed by Pb–In–Se is based on the remarkably distorted PbSe^{100} structure because of the strong influence of the lone-pair effect of Pb^{2+} . The Pb atoms show the triangular-prism coordination with two additional ligands; each coordination number is 8, and a one-dimensional Pb–Se unit is formed running parallel to the b axis. Average

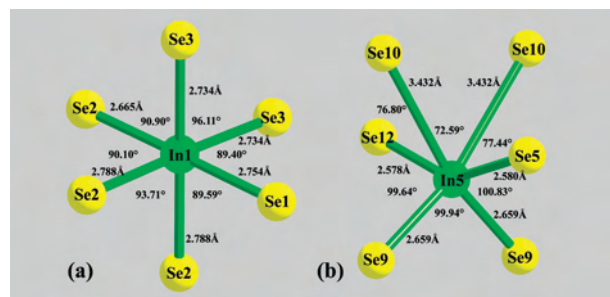


Figure 1. In coordination in **1**: (a) nearly regular octahedron coordination (In1–3 and 7–9); (b) remarkably distorted octahedron coordination (In4–6).

Pb–Se distances are 3.214 Å (Pb1), 3.214 Å (Pb2), 3.228 Å (Pb3), and 3.221 Å (Pb4), respectively. This coordination type of Pb atom is commonly found in complex Pb multinary chalcogenides.^{8–10,12,19} In atoms in slab B show a specific coordination type. One is regular octahedral coordination (In3 and In7) with average In–Se distances 2.784 Å (In3) and 2.759 Å (In7) (Figure 1a). Another type is remarkably distorted coordination (In4–6) that is formed by four shorter In–Se distances than 2.7 Å and two longer distances over 3.2 Å without any In–cation distances. These sites locate at the center in slab B.

Each of the average In–Se distances calculated as octahedra are 2.889 Å (In4), 2.890 Å (In5), and 2.843 Å (In6), respectively (Figure 1b). This specific distortion mode of this In coordination caused by the strong influence of the lone-pair electrons of stereochemically active Pb^{2+} is also found in the structures of **2**¹⁰ and $\text{Pb}_{7.12}\text{In}_{18.88}\text{Se}_{34}$.¹² However, we are convinced that the charge valences of these In atoms are lower than 3+ to keep the total charge neutrality of **1**. Even if In^+ is partially occupied at these sites, these distortion modes are reasonable because In^+ has stereoactive lone-pair electrons ($5s^2$).²⁰

Fe atoms are partially substituted at In sites with various Fe/In ratios: 9.5:90.5 at In2, 5.1:94.9 at In4, 4.6:95.4 at In5, and 4.1:95.9 at In8. These substitution behaviors are also observed in $\text{Fe}_{5.5}\text{Pb}_{5.5}\text{In}_{10}\text{S}_{22}$ ⁹ and **2**.¹⁰ However, the substitution feature of **1** is complex compared with the isostructure **2**. In the case of **2**, two of the In sites in three crystallographically independent In sites at slab B are disordered, and the transition metals are partially occupied at these disordered In sites. Another In site is fully occupied by an In atom. On the other hand, there is no disordered In site in **1**. Moreover, the Pb partially substitutes at In3, and a vacancy exists at In7. These sites locate between each Pb–Se unit in slab B. Moreover, they work not only as space-filling sites but also as charge neutralizers. Fe atoms are also substituted at In2 and In8 sites in slabs A and C. These sites are located at the connected parts in ribbon structures. These effects ease a structural distortion from an ideal PbSe -type structure in slab B caused by the strong influences of the stereoactive lone-pair effects of Pb^{2+} .

(12) Eddike, D.; Ramdani, A.; Brun, G.; Liautard, B.; Tedenac, J. C.; Tillard, M.; Belin, C. *Eur. J. Solid State Inorg. Chem.* **1997**, *34*, 309.

(13) (a) Eddike, D.; Burn, G.; Tedenac, J. C.; Ramdani, A.; Liautard, B. *J. Chim. Phys.-Chim. Biol.* **1997**, *94*, 1101. (b) Daouchi, B.; Record, M. C.; Tedenac, J. C. *J. Alloys Compd.* **2000**, *296*, 229. (c) Record, M. C.; Ilyenko, S.; Daouchi, B.; Tedenac, J. C. *J. Alloys Compd.* **2001**, *316*, 239.

(14) Compositional analyses were carried out using EDS analyses using a JEOL JSM-5600 scanning electron microscope at a 15-kV accelerating voltage and a 1-min accumulation time per one position in which the corrections were made for atomic number, absorption, and fluorescence. The following standards were used to calibrate each of the energies: metal Fe (Fe K α), PbSe (Pb M α and Se L α), and InSb (In L α).

(15) DTA was performed with a MacScience TG-DTA 2000 thermal analyzer. The ground samples were sealed in quartz ampules under vacuum. A quartz ampule containing $\alpha\text{-Al}_2\text{O}_3$ of almost equal mass was sealed and used as the reference. The samples were heated to 1273 K at 10 K/min and then isothermed 5 min followed by cooling at 10 K/min to room temperature. This process was repeated three times. After DTA measurements, the samples were rechecked by XRD.

(16) Intensity collection for the crystal structural analysis was carried out on a Rigaku R-AXIS RAPID imaging-plate-based single-crystal diffractometer (Mo K α radiation, 46 kV, 36 mA) at 295 K.

(17) Data for **1**: $\text{Fe}_{0.47}\text{In}_{17.37}\text{Pb}_{8.04}\text{Se}_{34}$, $M_r = 6371.12$, $P2_1/m$, $a = 13.2098(2)$ Å, $b = 4.06725(4)$ Å, $c = 28.3909(3)$ Å, $\beta = 94.6427(3)^\circ$, $V = 1520.36(3)$ Å³, $Z = 1$, $D_c = 6.959$ g cm⁻³, $F_{000} = 2679$, $\mu(\text{Mo K}\alpha) = 49.070$ cm⁻¹. $R = 0.0299$, $wR = 0.0581$ with $I > 2\sigma(I)$.

(18) Adenis, C.; Olivier-Fourcade, J.; Jumas, J. C.; Philippot, E. *Rev. Chim. Miner.* **1986**, *23*, 735.

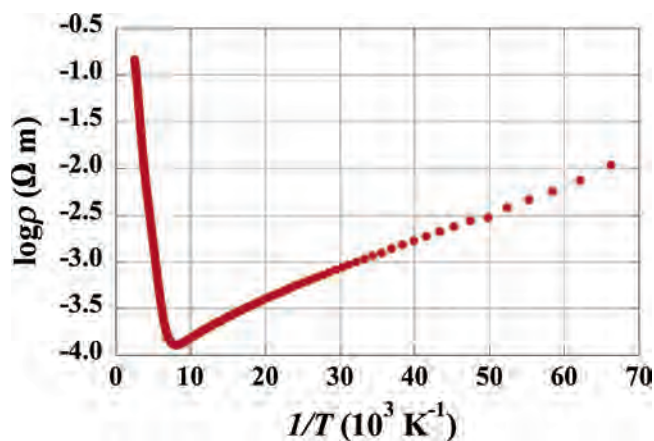


Figure 2. Inverse temperature dependence of logarithmic electrical resistivity of a single crystal of **1**.

From the coordinated feature of these Fe-substituted sites, the Fe seems to be taking a high-spin Fe^{2+} state, and the substituted Fe atoms do not seem to influence the crystallochemical features (coordination type, average bond length, average bond angle, and coordination volume) of these In sites. This substitution behavior is consistent with $\text{Fe}_{5.5}\text{Pb}_{5.5}\text{In}_{10}\text{S}_{22}^9$ because ionic radii [In^{3+} ($r_{\text{In}^{3+}}^{\text{CN}=6} = 0.80 \text{ \AA}$) and Fe^{2+} ($r_{\text{Fe}^{2+}}^{\text{CN}=6, \text{HS}} = 0.780 \text{ \AA}$)] and their bonding nature are very close.²¹ Therefore, from these crystallochemical features and synthetic results, the Fe atom seems to be an essential element to stabilize this type of structure, the same as Fe^{2+} in $\text{Fe}_{5.5}\text{Pb}_{5.5}\text{In}_{10}\text{S}_{22}^9$ and isostructure sulfide M^+ ($\text{M}^+ = \text{Cu}, \text{Ag}, \text{Au}$) in **2**.¹⁰ Because of a previous report on the failure of synthesized $\text{M}^+\text{Pb}_8\text{In}_{17}\text{Se}_{34}$ ($\text{M}^+ = \text{Cu}, \text{Ag}, \text{Au}$),¹⁰ the divalent transition metals may be suitable for stabilizing this type of structure in selenide.

The electrical resistivity (ρ) is as low as $\sim 0.025 \text{ \Omega m}$ at 300 K ²² (Figure 2). This value suggests that **1** is called a bad metal.²³ ρ is $\sim 0.15 \text{ \Omega m}$ at 400 K , and its temperature dependence shows three specific behaviors. As a first part in the temperature range $400\text{--}180 \text{ K}$, ρ gradually decreases with a decrease in the temperature down to $\sim 180 \text{ K}$ ($\sim 0.0007 \text{ \Omega m}$). The temperature range of the second region is $180\text{--}40 \text{ K}$. In this region, it shows almost a flat temperature dependence with a small minimum point of ρ_{min} , 0.00013 \Omega m at 120 K . Below 40 K , it increases rather sharply and reaches $\sim 0.02 \text{ \Omega m}$ at 15 K . These temperature dependences of resistibility in the first and second regions

are metallic behavior. This behavior suggests that the conduction electrons start to not move thermally below the 40 K region, and the point at 120 K is considered as the metal–insulator (or semiconductor) transition point of **1**. Therefore, the temperature dependence of ρ in this temperature region is the same as that of the semiconductor behavior having a narrow band gap. The estimated band gap (E_a) from an Arrhenius plot using data below 120 K is 0.078 eV . This value is much lower than that of PbSe (0.27 eV).²³ Thus, this narrower E_a range should be considered as the band gap between the impurity band formed by Fe substitution at In sites and the conduction (or valence) band.

Magnetic properties of this compound show a non-temperature-dependent paramagnetic.²⁴ The Weiss constant estimated from the Curie–Weiss fitting is 15 K . The effective magnetic moment, p_{eff} , estimated from C , is $4.72 \mu_B$, which suggests that Fe^{2+} takes a high-spin state ($t_{2g}^4 e_g^2$, $S = 2$) in this compound, although it is slightly lower than the calculated p_{eff} ($4.90 \mu_B$) for a high-spin Fe^{2+} .²⁵ These results indicate that **1** has a weak ferromagnetic interaction among the Fe^{2+} ions but is paramagnetic at least down to 2 K without any magnetic orderings.

In summary, we obtained the first M–Pb–In selenide example, **1**, that is evolved from the new structure-type phase by the partially occupied small amount of a divalent transition metal (Fe) at In sites. The crystal structure forms by three kinds of PbSe related slab structures. The In atoms have two specific coordination types; one is nearly regular octahedral coordination octahedron, and the other is remarkably distorted octahedral coordination octahedron. From the crystallochemical point of view, it seems that monovalent In atoms partially occupied at the latter coordination site to maintain total charge neutrality. The Fe atoms are partially substituted at In sites with various ratios. This substituted feature is consistent within our previously reported $\text{Fe}_{5.5}\text{Pb}_{5.5}\text{In}_{10}\text{S}_{22}$. **1** shows relatively high conductivity as a semiconducting material with a narrow-band-gap-type property. From the crystallographic point of view and transport properties with a very narrow band gap, **1** seems to have a potential for thermoelectric application.¹ From the results of magnetic susceptibility measurements, the ionic valence of Fe is $2+$ and the dominant interaction is weak ferromagnetic.

Acknowledgment. This work is partly supported by Grants-in-Aid for Scientific Research (Grants 407 and 758) and Creative Scientific Research (Grant 13NP0201) from the Ministry of Education, Culture, Sports, Science, and Technology. We also gratefully acknowledge Komatsu Ltd. for financial support.

Supporting Information Available: Crystallographic information file (CIF) for $\text{Fe}_{0.47}\text{Pb}_{8.04}\text{In}_{17.37}\text{Se}_{34}$ and Figure S1. This material is available free of charge via the Internet at <http://pubs.acs.org>.

IC0611600

- (19) (a) Ginderow, D. *Acta Crystallogr.* **1978**, *B34*, 1804. (b) Krämer, V.; Berroth, K. *Mater. Res. Bull.* **1980**, *15*, 299. (c) Krämer, V. *Acta Crystallogr.* **1986**, *C42*, 1089. (d) Krämer, V. *Acta Crystallogr.* **1983**, *C39*, 1328. (e) Krämer, V.; Reis, I. *Acta Crystallogr.* **1986**, *C42*, 249. (f) Matsushita, Y.; Takéuchi, Y. *Z. Kristallogr.* **1994**, *209*, 475. (g) Skowron, A.; Boswell, F. W.; Corbett, J. M.; Taylor, N. J. *J. Solid State Chem.* **1994**, *112*, 251. (h) Emirdag-Eanes, M.; Kolis, J. W. *Z. Anorg. Allg. Chem.* **2002**, *628*, 10.
- (20) van der Vorst, C. P. J. M.; Verschoor, G. C.; Maaskant, W. J. A. *Acta Crystallogr.* **1978**, *B34*, 3333.
- (21) Shannon, R. D. *Acta Crystallogr.* **1976**, *A32*, 751.
- (22) The dc electrical resistivity along the b axis of a single crystal was measured using a conventional four-probe method. The electrodes, ϕ 25-mm Au wires, were attached to the crystal by a Au paste. Measurements were carried out in the temperature range of $10\text{--}400 \text{ K}$ by a Quantum Design PPMs with an ac transport controller.
- (23) Berger, L. I. *Semiconductor Materials*; CRC Press: Boca Raton, FL, 1997.

- (24) Magnetic susceptibility measurements for pure polycrystalline samples were measured in the temperature range of $2\text{--}300 \text{ K}$ and an applied magnetic field of 0.5 T with zero-field cooling mode by using a Quantum Design 5T-MPMS SQUID magnetometer.
- (25) West, A. R. *Solid State Chemistry and Its Applications*; John Wiley & Sons: Chichester, U.K., 1984.